Biochimica et Biophysica Acta 1818 (2012) 636–644

Contents lists available at SciVerse ScienceDirect

Biochimica et Biophysica Acta

journal homepage: www.elsevier.com/locate/bbamem

Effects of the pore-forming agent nystatin on giant phospholipid vesicles

Luka Kristanc [a,*], Saša Svetina [a,b], Gregor Gomišček [a,c]

[a] Institute of Biophysics, Faculty of Medicine, University of Ljubljana, Ljubljana, Slovenia
[b] Jožef Stefan Institute, Ljubljana, Slovenia
[c] Faculty of Health Sciences, University of Ljubljana, Ljubljana, Slovenia

ARTICLE INFO

Article history:
Received 21 June 2011
Received in revised form 9 November 2011
Accepted 30 November 2011
Available online 8 December 2011

Keywords:
Nystatin
Giant phospholipid vesicle
Transmembrane pore

ABSTRACT

The effects of the polyene pore-forming agent nystatin were investigated on individual giant unilamellar phospholipid vesicles (GUVs), made of 1-palmitoyl-2-oleoyl-sn-glycero-3-phosphocholine (POPC), in different methanol–water solutions using phase-contrast optical microscopy. Three characteristic effects were detected in three different nystatin concentration ranges: vesicle shape changes (between 150 and 250 μM); transient, nonspecific, tension pores (between 250 and 400 μM); and vesicle ruptures (above 400 μM). Both the appearance of the transient tension pores and the vesicle ruptures were explained as being a consequence of the formation of size-selective nystatin channels, whose membrane area density increases with the increasing nystatin concentrations. Our results also show that nystatin is able to form pores in the absence of sterols. In addition, study of the cross-interactions between nystatin and methanol revealed mutually antagonizing effects on the vesicle behavior for methanol volume fractions higher than 10%.

1. Introduction

Polyene antibiotics are a class of biologically active bacterial metabolites isolated from *Streptomyces*, an aerobic actinomycete genus obtained from soil. While more than one hundred polyene antibiotics have been described, amphotericin B (AmB) and nystatin are the two agents most commonly used to treat fungal and protozoal infections in humans [1]. In fact, AmB has been the most common antifungal agent used to treat invasive systemic fungal infections in critically ill patients over the past 50 years. This can be ascribed to its wide spectrum of activity towards pathogenic fungi in comparison to many other antifungal compounds, e.g., azoles [2,3]. However, several side effects, especially nephrotoxicity and hepatotoxicity, have limited its use. In order to minimize these problems, various liposomal formulations were developed [4]. In contrast to AmB, the use of nystatin is currently limited almost exclusively to the topical treatment of superficial Candida infections, since it is not effective when given orally and is severely toxic as an intravenous application [4]. Nevertheless, nystatin has recently been successfully incorporated into liposomal pharmaceutical formulations, which reduced its toxicity dramatically without losing its therapeutic properties [5,6]. It has been shown that the antifungal activity of nystatin is broader in comparison to AmB and could, therefore, be more effective when given by the intravenous route [7]. As a pore-forming agent, nystatin could also be capable of translocating different cargo molecules into the cells, which makes it a potential specific drug-delivery agent [8]. Therefore, in order to develop even more acceptable nystatin formulations, it is essential to know in greater detail its mode of action at the membrane level.

The biological target for polyene action is the plasma membrane of the antibiotic-sensitive organisms, where polyenes are believed to exert their function through the formation of barrel-like, membrane-spanning channels [1,9,10]. Several electrophysiological studies have shown that bilayer-spanning, potassium-selective channels are formed after the one-sided addition of nystatin or AmB to different lipid membranes [11]. These pores have size-selective properties, being permeable only to solutes not larger than glucose, in the case of nystatin, or sucrose, in the case of AmB [12,13]. The disturbance of the cellular electrochemical gradients, caused by the increase of the plasma-membrane permeability to ions and small molecules, ultimately leads to cell lysis and death [1]. Bacteria have membranes that are completely devoid of sterols and are insensitive to polyene antibiotics. In relation to this, it was proposed that their mode of action must be in some way connected to the sterols in the membrane [14–18]. Consequently, many different molecular models describing the role of sterols have been presented, including the formation of specific antibiotic-sterol complexes [10,19–21] and/or an increased membrane partition of polyene antibiotics due to a change in the overall membrane lipid organization influenced by sterols [22,23]. The exact molecular mechanisms have, however, not been resolved yet. The problems are even more complex if, in addition, the influence of the membrane phospholipid composition on the pore-forming effect of polyenes is considered [24,25]. Furthermore, it has

* Corresponding author at: Institute of Biophysics, Faculty of Medicine, University of Ljubljana, Lipičeva 2, 1000 Ljubljana, Slovenia. Tel.: +386 1 5437600, +386 40 566 950(gsm); fax: +386 1 5437601.
E-mail address: luka.kristanc@gmail.com (L. Kristanc).

0005-2736/$ – see front matter © 2011 Elsevier B.V. All rights reserved.
doi:10.1016/j.bbamem.2011.11.036

been shown, in contrast to earlier observations [19–23], that polyenes are also able to form pores in membranes that do not contain any sterols [26–29].

Extensive research efforts have been made in the area of the polyene molecular activities exerted on lipid bilayers of small unilamellar vesicles (SUVs) and large unilamellar vesicles (LUVs) [10,26,30,31]. The bulk properties of the membrane-polyene interactions were primarily studied using different fluorescent techniques [10,30,31]. In contrast to this, there is a lack of research on single vesicles with dimensions more comparable to the size of an average human cell, i.e., research on giant unilamellar vesicles (GUVs).

In this article we report on studies focusing on individual GUVs, which reveal the characteristic behavior patterns of lipid vesicles when exposed to nystatin at different concentrations. Our vesicles were made solely out of 1-palmitoyl-2-oleoyl-sn-glycero-3-phosphocholine (POPC) which was chosen due to its abundance in biological membranes and its chemical characteristics. Its gel-fluid phase transition temperature at about −2.6 °C [32] makes it appropriate for the studies in the fluid phase, which is characteristic for the lipids in biological membranes. In addition, POPC is one of the most commonly used phospholipids which enables an easier comparison to other studies. The GUVs, selected and manipulated by the micropipette technique under phase-contrast microscopy, demonstrated complex concentration-dependent interactions with the nystatin. In addition, as methanol is commonly used as a cosolvent for nystatin in experimental procedures, we dealt in some detail with the interactions of methanol and nystatin at the lipid-membrane level.

2. Materials and methods

2.1. Preparation of vesicles (GUVs) and nystatin stock solutions

The GUVs were prepared from POPC (Avanti Polar Lipids, USA) according to the modified method of Angelova et al. [33] in a 0.2 M sucrose solution with a pH of 7.5. The lipid (POPC) was dissolved in a chloroform–methanol mixture (1:1, vol/vol), spread over wire platinum electrodes and then vacuum dried. The electrodes were placed in an electroformation chamber, filled with 2 ml of sucrose solution. An AC field of 1 V/mm and 10 Hz was applied for 2 hours, afterwards reduced to 0.5 V/mm and 5 Hz for 15 min, and then 0.25 V/mm and 2 Hz for the next 15 min. Finally, an AC field of 0.1 V/mm and 1 Hz was applied for 30 min. The vesicles formed with the entrapped sucrose solution were transferred to an isomolar glucose solution and were kept at 4 °C. The samples were used within 3 days of preparation.

Stock solutions of 1 mM and 10 mM nystatin were prepared using lyophilized nystatin (Fluka, Sigma, USA) and stored at −20 °C in a dark place. Pure methanol was used as a solvent due to the poor solubility of nystatin in water. Before the experiment, the stock solutions were stirred using a magnetic stirrer and diluted with 0.2 M glucose solution in order to obtain nystatin solutions with the desired concentrations.

2.2. Observation and manipulation of vesicles

The effects of nystatin on the giant phospholipid vesicles were observed using phase-contrast microscopy. An inverted microscope (IMT-2, Olympus, Japan; objective LWD CDPlan40X, NA = 0.55) was used. The images were continuously acquired with a chilled black-and-white CCD camera (C5985, Hamamatsu, Japan) and recorded on a video recorder (VCR, Sony, SVO-9500 MDP, Japan). The images selected for the quantitative determination were also digitized using an 8-bit frame grabber (DT 2851, Data Translation Inc., USA) and stored in a personal computer. All the images were processed and analyzed using in-house-produced software.

A two-compartment cell was used to select and transfer the individual vesicles. One compartment was filled with the prepared vesicle solution, while the other, measuring compartment, was filled with isomolar glucose solution and nystatin in the desired concentrations. The sugar concentrations were equal to 0.2 M in both compartments. The volume of the measuring compartment was around 80 μl. Individual unilamellar, nearly spherical vesicles with a diameter of approximately 40 μm were chosen and transferred in groups of 1 to 5 vesicles into the measuring compartment using a micropipette manipulation system. Since the volume of the transferred solution was much smaller compared to the volume of the measuring compartment, the concentration in the measuring compartment remained practically constant. Due to an open measuring compartment and the water evaporation associated with it, small changes in glucose concentration occurred during the measurement. As a consequence, minor fluctuations of the vesicle could be observed at the end of the measuring period in control experiments and at low nystatin concentrations. The measurements were performed at a controlled room temperature of 23 ± 1 °C and at a constant pH of around 7.5.

2.3. Experimental procedures

The response of the GUVs to nystatin in concentrations between 10 and 1000 μM was studied in two separate sets of experiments. In the first set the methanol was maintained at volume fractions under 10% in order to minimize its effects (the methanol fraction was increased by 1% as the nystatin concentration was increased by 100 μM). In the second set of experiments, in contrast, the combined effects of methanol and nystatin were investigated. For this purpose the methanol volume fraction was increased by 10% as the nystatin concentration was increased by 100 μM, making it possible to observe their interactions at methanol volume fractions between 10% and 75%. In addition, the experiments with methanol at low (under 10%) and at high volume fractions (above 10%) without nystatin were performed.

Each time before the GUVs were exposed to nystatin and/or methanol, control experiments testing the stability of the GUVs were conducted by the transfer of intact vesicles into the isomolar glucose solution. In an initial set of experiments, we also thoroughly tested the influences of the micromanipulation procedure itself on the vesicle's behavior.

2.4. Analysis of the images

The obtained images were analyzed on the qualitative and quantitative levels. Qualitatively, an assessment was made of the characteristic vesicle behavior patterns at different nystatin concentrations. This was based on a continuous observation of the phase-contrast images within the first 60 min after the vesicle transfer. The images of the vesicle were kept focused in the equatorial plane. The quantitative analysis of the images was accomplished as follows. In positive phase-contrast microscopy the halo intensity depends on the difference between the refractive indices of the solutions inside and outside the vesicle, the size of the vesicle and the properties of the microscope [34]. The intensity was assessed using the brightness profile along the line across the vesicle membrane in a radial direction, which was fitted across the halo region by a Gaussian curve [35]. Since for a constant vesicle size the halo intensity depends solely on the difference between the refractive indices, the determined halo intensity was used as a measure of the changing sucrose-glucose ratio inside the vesicle. This was possible since the refractive index of a sucrose solution is higher than that of a glucose solution of the same concentration. The quantitative results were evaluated using standard statistical procedures.

3. Results

3.1. Studying the effects of nystatin on the GUVs

The primary goal of our experiments was to study the effects of nystatin at different concentrations on the GUVs made from POPC. The results show that the characteristic behavior of the GUVs changed

significantly as the nystatin concentrations increased. As a rough subdivision, four different, partially overlapping, nystatin concentration ranges were selected with respect to the vesicle response:

- range A (concentrations up to 150 μM),
- range B (concentrations between 150 and 250 μM),
- range C (concentrations between 250 and 400 μM),
- range D (concentrations above 400 μM).

For range A no significant changes in the vesicle behavior were detected in comparison to the control experiments. The vesicles remained spherical and stable with no significant changes in the size, phase contrast and halo intensity over a period of 1 hour (Figs. 1a and 2). Minor fluctuations of the vesicles were observed at the end of the measuring period.

For the concentration range B, after they were transferred into the measuring compartment, the vesicles also remained spherical for a few minutes. Later, various membrane formations evolved gradually, which were predominantly oriented to the exterior of the vesicles. Their shapes and sizes were quite diverse, ranging from thin or thick filamentous formations, named tethers, which usually transformed into necklace-shaped rows of minute spheres, to disorganized groups of spheres, which often extended over the majority of the vesicle surface (Fig. 1b). However, the most commonly observed formations were relatively short, thick, external tethers and small spheres, slowly growing over time. On occasions, we noticed shape transformations involving changes in the number of spheres, e.g., by merging with the mother vesicle. The halo intensity of the vesicles was found to fall by about 30% with respect to the initial intensity (Table 1 and Fig. 2). The rate of decrease was approximately $-7.1\times10^{-5}\,s^{-1}$ during the first 10 min. Afterwards, the fading process increased and the halo intensity dropped to approximately 75% of the initial value at a rate of $-1.3\times10^{-4}\,s^{-1}$. After 35 min the fading process slowed and then continued at a rate of about $-1.2\times10^{-5}\,s^{-1}$ (Table 1).

For the concentration range C the existence of three different sequential fading phases was also observed (Fig. 2), however, with a significantly shorter duration of the first phase (a few tens of seconds). The vesicles also demonstrated an approximately 10-fold higher rate of halo intensity decrease compared to the concentration range B (Table 1 and Fig. 2) and an almost complete loss of halo intensity (Table 1 and Fig. 1c, 2). Many transient bursts, not observed in range B, were detected at regular time intervals, which lasted about one second (Fig. 3). They could be seen only when they were formed in proximity to the focal plane of the vesicle and they seemed to always appear at the same location with respect to the vesicle membrane. Membrane formations were, in contrast to concentration range B, seldom seen.

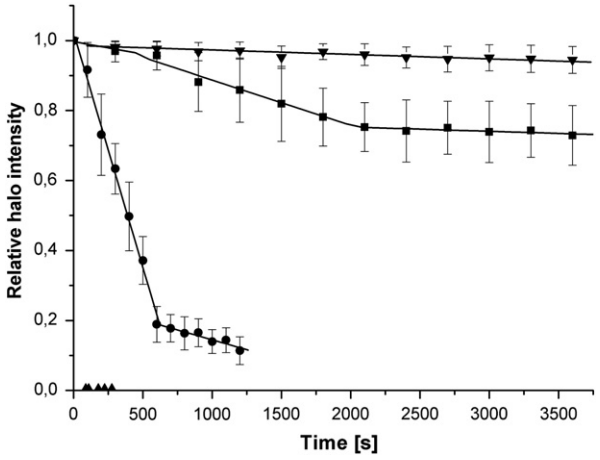

Fig. 2. Typical relative halo-intensity decrease at different nystatin concentration ranges and low methanol volume fractions: 100 μM nystatin ($n=9$, 1% methanol) (▼), 200 μM nystatin ($n=7$, 2% methanol) (■) and 300 μM nystatin ($n=8$, 3% methanol) (●). Halo-intensity values are normalized with respect to the initial halo-intensity value of the individual vesicles. Data are fitted by three linear fits representing different fading phases, the first phase cannot be shown at high nystatin concentrations (range C) due to its short duration. Vertical bars represent standard deviations. Average vesicle survival times at ≥400 μM nystatin ($n\approx40$; 4%≤methanol<10%) (▲) are added for comparison.

The characteristic phenomena for the concentrations above 400 μM (range D) were vesicle ruptures, denoting a quick disintegration of the entire vesicle. These ruptures were usually preceded by the formation of individual or multiple, well-localized bulges in the membrane and only occasionally by a partial loss of halo intensity. Regarding the

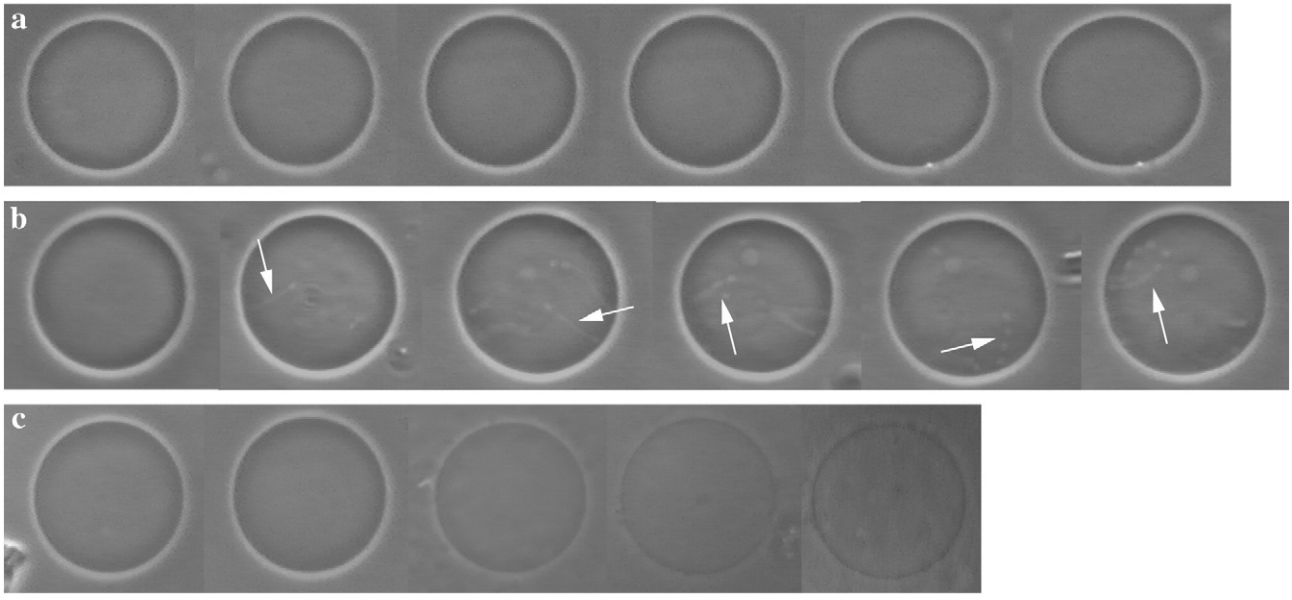

Fig. 1. Characteristic vesicle behavior for nystatin concentration ranges A, B and C (see text for descriptions): a) The snapshots were taken at 10-min intervals. The behavior of the GUVs (nystatin concentration was 100 μM) was identical to the control experiments. b) The snapshots were taken at 4, 28, 32, 37, 45 and 48 min after the vesicle transfer into the 200 μM nystatin solution. Arrows indicate typical structures, gradually evolving from predominantly thin tethers at the beginning to spherically shaped necklaces towards the end of the observation. Note the absence of these structures on the first image. c) The sequence of snapshots taken at 1, 3, 7.5, 9.5 and 10.5 min after the vesicle transfer into the 300 μM nystatin solution. The diameter of all vesicles was around 30 μm.

Table 1
Comparison of major characteristics of the fading process for nystatin concentration ranges B and C at low methanol volume fractions.

Range	Halo intensity decrease						Final halo intensity [% of initial]
	First phase		Second phase		Third phase		
	Rate [10^{-4} s^{-1}]	Duration [min]	Rate [10^{-4} s^{-1}]	Duration [min]	Rate [10^{-4} s^{-1}]	Duration [min]	
B	−0.71	10	−1.3	35	−0.12	15	73
C	−5.3	0.6	−13	10	−1.1	10	11

mode and duration of the vesicle disintegration, three types of ruptures were observed: fast ruptures (explosions), slow (partial) ruptures and "stable-opening" ruptures.

Fast ruptures or explosions were the most commonly detected type of ruptures. The vesicle membrane suddenly opened and the vesicle, which seemed intact just a fraction of a second ago, simply disappeared, leaving no visible traces behind (Fig. 4a). The incidence of explosions was found to increase with increasing nystatin concentrations in the solution. Slow or partial ruptures were also frequently observed. The membrane of the vesicle opened for a fraction of a second and a significant part of its content leaked out (Fig. 4b). Later, the membrane resealed. The diameter of the vesicle was found to be considerably reduced (at least by one third). This cycle of membrane opening and resealing was repeated several times, until the vesicle disintegrated into lipid debris. Such slow ruptures occurred preferentially at nystatin concentrations of approximately 500 μM. The third type of rupture was characterized by a stable opening with a distinctive orifice (Fig. 4c). Firstly, a few dark spots or bulges appeared on the vesicle membrane. They gathered to form the orifice of a stable opening, through which the sluggish emptying of the vesicle content began. The diameter of the vesicle gradually decreased, but, on the other hand, the diameter of the stable opening remained almost constant during the entire emptying process, which lasted for a few seconds. During this process the excessive membrane gathered around the opening, forming an amorphous relict of the vesicle at the end. This type of rupture was extremely rare.

In order to get a more complete picture, we should have a more quantitative look at certain aspects in relation to vesicle ruptures. The survival time of the vesicles, which denotes the time from the vesicle transfer into the nystatin solution to the vesicle rupture, decreased as the nystatin concentration increased (Fig. 5, dashed line). The slope of the linear regression line corresponds to a 55 s decrease of the survival time per 100 μM of nystatin-concentration increase. The predominant type of vesicle rupture at nystatin concentrations between 400 μM and 600 μM was observed to be slow ruptures, while explosions were the most frequently observed type at concentrations above 600 μM. The occurrence frequencies of the explosions were 11%, 29%, 70% and 90% at 400 μM, 500 μM, 600 μM and 700 μM nystatin concentrations, respectively.

3.2. Control experiments (without nystatin) with low and high methanol volume fractions

As methanol was used as a solvent for nystatin in the experimental procedures, we decided to conduct a series of control experiments with methanol (without nystatin) in different volume fractions in the solution surrounding the GUVs.

The control experiments with no methanol showed that a mechanical stress imposed on the vesicles during the micromanipulation procedure does not affect the behavior of the vesicles to a measurable extent. During the entire measuring period, neither significant shape changes nor halo-intensity decrease were detected (like in Figs. 1a and 2). Furthermore, the transfer of vesicles into glucose-methanol solutions with methanol at volume fractions not exceeding 10% did not cause any detectable changes.

However, the results of the experiments with methanol volume fractions higher than 10% differed significantly. At a 25% methanol volume fraction the GUVs started to fade approximately 5 min after the transfer. Their relative halo intensities decreased to about 10% of the initial value in the following 20 min at a rate of $-7.6\times10^{-4}\,s^{-1}$. Similarly, a decrease of the halo intensity was observed for the 50% and 75% methanol volume fractions, the average halo-intensity decrease rates being seven and seventeen times higher than the rates for the 25% methanol volume fraction, respectively (Fig. 6). Several transient membrane bursts were also observed at all these methanol fractions. In addition, for the 50% and 75% methanol volume fractions the vesicle diameters gradually decreased over time. During the course of this process, lipid aggregations were seen in the proximity of the membrane bursts.

3.3. High methanol volume fractions with significant nystatin/methanol cross-interactions

A methanol volume fraction of 10% was taken as the reference between the low and high methanol volume fractions, since it is approximately the volume fraction at which the transition of the membrane phospholipids from the non-interdigitated to the interdigitated state occurs [36]. Analogously with experiments at low methanol volume fractions, the same four characteristic, nystatin-concentration-dependent vesicle behaviors were observed for high methanol volume fractions. However, the nystatin concentration intervals of the four characteristic ranges were found to be shifted by 50–100 μM towards higher values: range A up to 200 μM, range B to concentrations between 200 μM and 350 μM, range C to concentrations between 350 μM and 500 μM and range D to concentrations above 500 μM. A comparable shift in the nystatin concentration between the low and high methanol volume fractions was also found in the measurements of the vesicle survival times (Fig. 5). Similarly, three different, successive fading phases were detected in concentration ranges B and C (Fig. 6). The relative halo-intensity decrease rates in ranges B and C

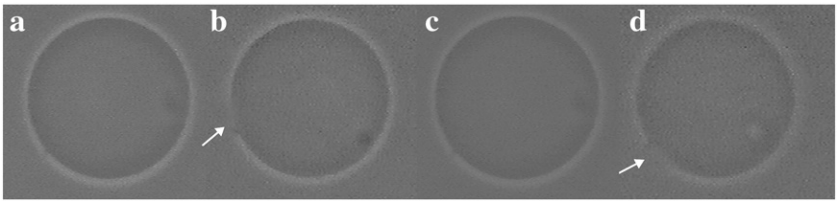

Fig. 3. Presentation of a typical burst encountered in range C (see text for a detailed explanation). a) Vesicle with a tensed membrane. b) Vesicle membrane opens transiently (arrow) and a minor fraction of the vesicle content is extruded out of the vesicle (seen as a light shadow). c) Vesicle with a resealed membrane and d) Vesicle membrane reopens (arrow).

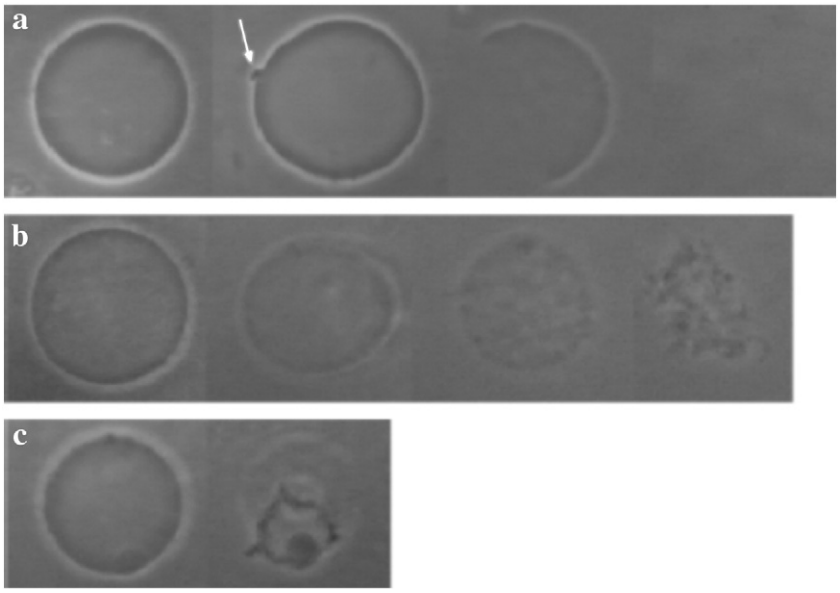

Fig. 4. Different types of vesicle ruptures (see text for descriptions): a) A typical fast rupture (explosion) of the vesicle. The first three snapshots were taken at 0.5, 2 and 2.5 min after the vesicle transfer into a 600 μM nystatin solution. The fourth snapshot was taken immediately after the third one. b) A typical slow (partial) rupture of the vesicle. The snapshots were taken about 6 min after the transfer into the 500 μM nystatin solution. Time intervals during the first three snapshots were approximately 1.5 s. c) A typical "stable-opening" rupture. The snapshot on the right was taken 5 min after the transfer of the vesicles into a 400 μM nystatin solution.

were comparable to the rates obtained for the low methanol fractions (Tables 1 and 2).

Some behavioral aspects were significantly different from those at low methanol volume fractions. For the concentration range B, extensive lipid networks were the predominant type of membrane formations (Fig. 7). In addition to the ruptures, another type of behavior was found for range D, i.e., the appearance of flaccid elongated vesicles. The vesicles became flaccid and attained an elongated shape in 140 s ± 50 s after their transfer; their membranes were fluctuating vividly and their halo intensity was usually almost completely lost (Fig. 8).

4. Discussion

Polyene–lipid membrane interactions have been, using different fluorescent techniques, extensively studied by employing small and large unilamellar vesicles (SUVs and LUVs) [10,30,31]. Our research was, in contrast to these studies (which could only be realized at the level of vesicle populations), focused on the behavior of individual giant vesicles. We were thus able to obtain a new insight into the mechanisms induced by nystatin activity at the lipid membrane level. Firstly, our results are consistent with the previous findings

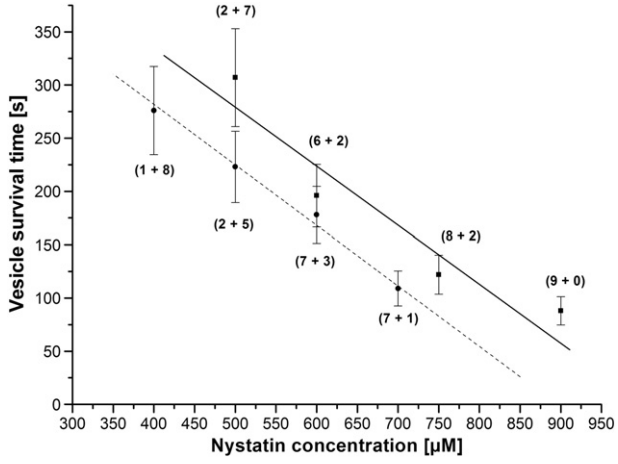

Fig. 5. The relationship between the survival time of the vesicles and the nystatin concentration at low methanol volume fractions (4%, 5%, 6% and 7%) (●) and at high methanol volume fractions (50%, 60%, 75% and 90%) (■) with the lines as a guide to the eye (– – low methanol volume fractions, — high methanol volume fractions). Methanol volume fractions are increasing along each line in accordance with the increasing nystatin concentrations. 7–10 vesicles were observed at each nystatin concentration; vertical bars represent the 95% safety interval. The occurrence of different types of ruptures is shown in parentheses (explosions + other types).

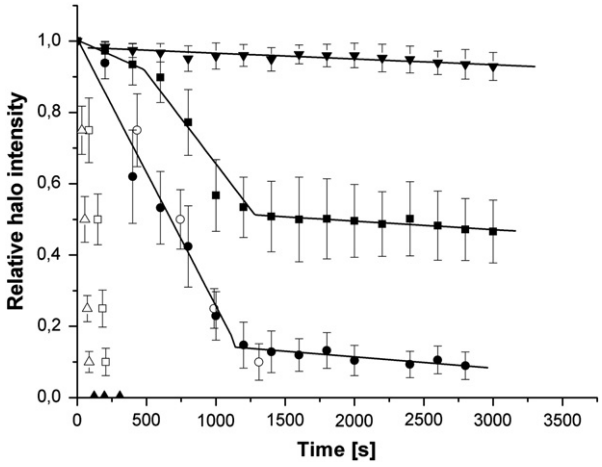

Fig. 6. Typical relative halo-intensity decrease at different nystatin concentration ranges and high methanol volume fractions: 100 μM nystatin ($n = 10$, 10% methanol) (▼), 300 μM nystatin ($n = 6$, 30% methanol) (■), 400 μM nystatin ($n = 7$, 40% methanol) (●). For comparison, open symbols depict the fading dynamics in control experiments with high methanol volume fractions (without nystatin): 25% methanol ($n = 8$) (○), 50% methanol ($n = 7$) (□) and 75% methanol ($n = 7$) (△). Halo-intensity values are normalized with respect to the initial halo-intensity value of the individual vesicles. Data are fitted by three linear fits representing different fading phases, the first phase cannot be shown at high nystatin concentrations (range C) due to its short duration. Vertical bars represent standard deviations. Average vesicle survival times at ≥ 500 μM nystatin ($n \approx 30$; ≥ 50% methanol) (▲) are added for comparison.

Table 2
Comparison of major characteristics of the fading process for nystatin concentration ranges B and C at high methanol volume fractions.

Range	Halo intensity decrease						Final halo intensity [% of initial]
	First phase		Second phase		Third phase		
	Rate [10^{-4} s^{-1}]	Duration [min]	Rate [10^{-4} s^{-1}]	Duration [min]	Rate [10^{-4} s^{-1}]	Duration [min]	
B	−1.7	10	−5.3	10	−0.29	30	46
C	−1.4	1.3	−7.8	16	−0.32	26	9

[26–29] that nystatin can form large pores even in the sterol-free POPC membrane (Table 1 and Figs. 1–5). Moreover, our observations show that this effect is not negligible and it could have an important role in membrane-permeability changes, which can lead to cell destruction (i.e., antifungal activity, side effects of treatment). Secondly, as presented in the Results section, three different, characteristic, concentration-dependent phenomena were revealed: *i*) vesicle shape changes and membrane formations at small concentrations (range B), *ii*) membrane bursts at intermediate concentrations (range C) and *iii*) vesicle ruptures at high concentrations (range D) of nystatin. It should be noted that the subdivision of the results into discrete concentration ranges is artificial and that it was made only with an intention to stress four distinctly different vesicle behavior patterns.

4.1. Vesicle shape changes and membrane formations

With respect to the different vesicle shape changes and membrane formations, which were observed in the concentration range B, a tendency to initially form thin tethers that was followed by their shape evolution into necklaces was predominantly observed. This behavior is consistent with the theories of membrane shape transformations [37,38] and the theory of pore formation [39–41]. According to the latter, a two-step process is involved in the formation of a pore: insertion of the pore-forming polypeptides on the lipid membrane in a horizontal orientation, followed by a repositioning into the membrane in a perpendicular direction. We may assume that the first step, the insertion of the nystatin molecules in the outer membrane monolayer in the horizontal direction, increases the area of the outer membrane monolayer compared to the inner one. In contrast, in the second step, the positioning of the nystatin molecules in the membrane in a perpendicular direction and their self-aggregation with pore formation, this increase is diminished. This is due to a significantly smaller surface area of the nystatin molecule positioned in a perpendicular direction relative to the horizontal one [42]. Nystatin molecules passing into the inner membrane monolayer could also be a reason for an additional decrease of the relative area difference between monolayers. Furthermore, the formation of pores (i.e., toroidal or "wormhole" pores) could enable a "pore-mediated flip-flop" [43], resulting in an enhanced flow of lipid molecules from the outer to the inner membrane leaflet causing a further diminishment of the previously increased leaflet-area difference. Thus, in accord with these mechanisms, the process of pore formation should be accompanied by an increase and, subsequently, a decrease of the area difference between both membrane monolayers. These descriptions can only be considered as qualitative, since the steps of the nystatin concentration changes in our experiments were too large to get quantifiable shape sequences. Future studies of GUVs shape changes focused only on this concentration range might reveal to be the most sensitive indicators of the subtle nystatin-membrane interactions.

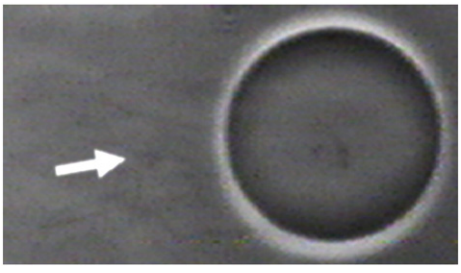

Fig. 7. Extensive membrane lipid networks (arrow) characteristic for nystatin concentration range B at high methanol volume fractions.

4.2. Membrane bursts and vesicle ruptures

The observed membrane bursts (tension pores) in range C and vesicle ruptures in range D can be understood as occurring due to an increase in the membrane tension to a critical level. The repetitive transient membrane bursts resemble the phenomena encountered previously (e.g., with equinatoxin II as a pore-forming agent) [35]. Increased membrane tension was attributed to the occurrence of osmotic stress in the vesicles after the transmembrane pores with a fixed diameter were formed. The transmembrane permeability due to nystatin pore-forming activity was found to have size-discriminating properties [44], leading to a higher permeability for glucose molecules with the radius $r_g \sim 0.38$ nm with respect to sucrose molecules with a larger effective hydrodynamic radius ($r_s \sim 0.52$ nm) [45]. Since, initially, the sucrose solution is inside and the glucose solution is outside the vesicle, the osmolarity in the vesicle is increasing, which induces an influx of water into the vesicle. It results in an increased volume of the vesicle, associated with an increased membrane tension and a corresponding hydrostatic pressure, which were confirmed by the model simulations of osmotically driven influx of water in similar experiments with equinatoxin II and melittin [35,46]. The membrane burst occurs when the membrane area reaches its critical value, corresponding to a membrane tension comparable to the estimated critical tension (rupture strength) of the lipid bilayers, which is, in dependence on the lipid composition and the rate of tension change, approximately 1–25 mN/m [47,48]. During the burst, the vesicle membrane opens transiently and a minor fraction of the vesicle content, including sucrose, is instantaneously and non-selectively extruded out of the vesicle (Fig. 3). The cycle of membrane opening (bursting) and resealing is repeated until the solutions inside and outside the vesicle are equalized. This mechanism explains a faster fading compared to the fading in range B (Table 1 and Figs. 1c, 2).

At nystatin concentrations beyond 400 μM (range D), different types of vesicle ruptures were encountered: slow ruptures, "stable-opening" ruptures and explosions. These processes could be attributed to a higher rate of transmembrane exchange of the sugar molecules due to a larger number of size-selective transmembrane pores and, consequently, a more intense water influx into the vesicle than in range C. If this flow exceeds a certain threshold value, the tension pore cannot be resealed anymore. Thus, the process becomes irreversible and is manifested as slow ruptures, characterized by a delayed resealing of the membrane after a loss of a greater quantity of the vesicle content (Fig. 4b), or "stable-opening" ruptures, represented by an opening with a constant diameter (Fig. 4c). At the highest nystatin concentrations even a delayed membrane resealing or a "stable opening" becomes impossible—explosions take place, which are revealed by

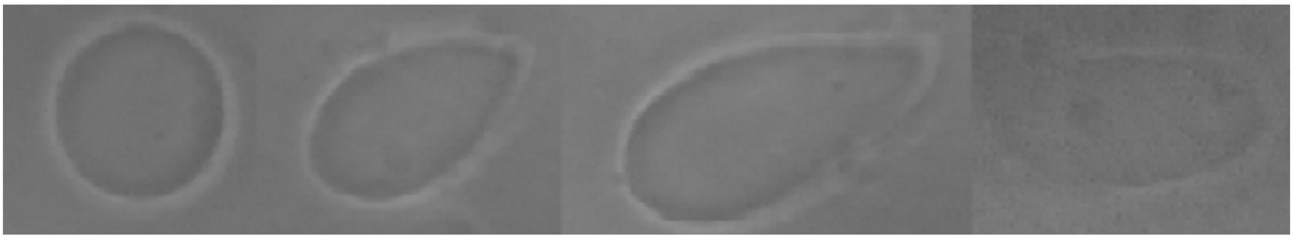

Fig. 8. The behavior of a vesicle at 1.1, 1.9, 2.7 and 3.7 min after its transfer to the 500 μM nystatin solution with a high (50%) methanol volume fraction (see text).

a total disintegration of the vesicle (Fig. 4a). In the studies with equinatoxin II, it was shown that the acceleration of the fading process with increasing equinatoxin II concentrations takes place mainly due to an increase of the surface density of the equinatoxin II transmembrane pores, while their diameter remains constant [35]. Our results suggest that this is also true in the case of nystatin and its transmembrane pores.

4.3. Implications of nystatin effects

Our findings demonstrate that both, the gradual content dissipation at lower nystatin concentrations as well as the almost instantaneous, total content dissipation at higher nystatin concentrations can be attributed to a single mechanism (cause), i.e., the formation of selective transmembrane pores by the nystatin molecules. Thus, the observations of single vesicles allow us to explain a two-stage model of the nystatin membrane permeabilization [30] by a single mechanism. The gradual content dissipation which is induced by the occurrence of the transient tension pores (membrane bursts) can be correlated to the first stage (the "graded" type) of membrane permeabilization and the fast, total content dissipation, induced by the vesicle ruptures, can be assigned to the second stage (the "all-or-none" type).

At this point it should also be made clear that the membrane bursts, as an alternative and non-selective mechanism of vesicle content exchange, do not need to be localized in the vicinity of the nystatin pores or other forms of self-aggregated nystatin molecules. We can assume that the membrane bursts occur at locations with the smallest bilayer resistance to an increased membrane tension (i.e., membrane failures or irregularities) that are not necessarily connected to nystatin molecules. Furthermore, we may even speculate that the mechanism for the halo-intensity decrease is the same in range B and in range C. But in contrast to range C, the membrane bursts should take place over much longer time intervals in range B and therefore, a ten times slower reduction of the halo intensity in range B is observed.

The phenomena observed in our measurements occurred at an approximately ten times higher nystatin concentration than those in the literature [10,30,31]. This may be attributed to a significantly larger diameter and, consequently, to the different physical characteristics of the GUVs used in our study in comparison to the LUVs or SUVs used in other studies. Probably the most important factor to be considered in this respect is that the volume of the GUVs is larger than that of the LUVs or SUVs. As a consequence, the processes depending on the vesicle volume-to-area ratio (i.e., the increase of the membrane tension) take longer periods of time or they need higher pore densities to be completed in comparable experimental times. The characteristic time before the onset of the vesicle burst is namely proportional to the ratio between the vesicle radius and the membrane permeability, which is dependent on the pore density [35]. In addition, a higher curvature radius of smaller vesicles causes a decreased packing density of the phospholipid molecules in the head region of the outer lipid monolayer, which can facilitate the first phase of the incorporation of nystatin into the vesicle membrane [49–51]. The shift towards higher nystatin concentrations can, moreover, be explained by the necessity of the larger transmembrane pores to enable the passage of sugar molecules with greater radii compared to different ions, e.g., potassium, used elsewhere [10,30,31]. It seems that the above mentioned arguments compensate the fact that there is less total membrane area in the measuring compartment in our experiments compared to those with LUVs and SUVs. The latter would namely imply a shift towards lower nystatin concentrations in the experiments with GUVs.

4.4. Effects of methanol and the influence of nystatin-methanol cross-interactions

As methanol had to be used in all our experiments as a cosolvent for the nystatin, control experiments with different methanol volume fractions (without nystatin) were carried out in order to elucidate the effects of methanol on the vesicle behavior. They revealed the significant influence of methanol alone only at more than 10% volume fractions: the occurrence of tension pores accompanied by a decrease of halo intensity (Figs. 6 and 9) and an observed decrease of vesicle diameters. Therefore, the cross-interactions between the nystatin and the methanol were assumed to be negligible in the interpretation of the experimental results, which were obtained with methanol volume fractions under 10%. This is in agreement with previous studies [10,30] performed at methanol volume fractions of less than 6%, where these cross-interactions have not been considered as a problem. However, for methanol volume fractions of greater than 10% in the medium surrounding the vesicles, the cross-interactions between the methanol and the nystatin became evident. In short, a significant shift of the concentration ranges towards higher nystatin concentrations (Figs. 2, 5, 6) shows that the methanol and nystatin membrane activities are mutually antagonizing (Fig. 9). By recalling also qualitative features, like the occurrence of extensive membrane networks and stable, extremely flaccid and elongated vesicle shapes detected at high nystatin concentrations (Figs. 7 and 8), we may

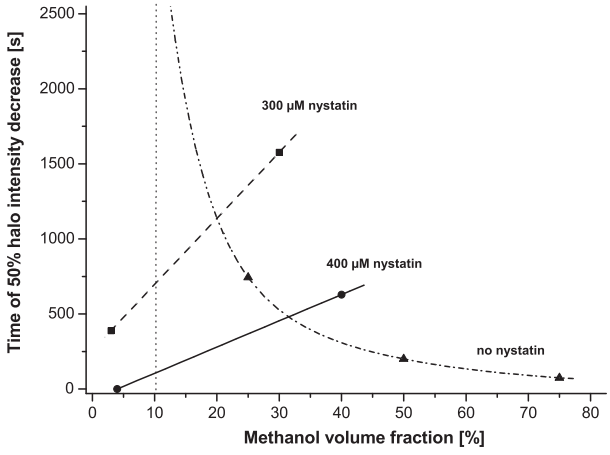

Fig. 9. Time of 50% halo-intensity decrease at different methanol volume fractions as a measure of nystatin-methanol cross-interactions: at zero (··—··, ▲), 300 μM (——, ■) and 400 μM (—, ●) nystatin concentration. The lines are drawn only as a guide to the eye. Asymptotic behavior of curve at zero nystatin concentration implies no halo intensity decrease at less than 10% methanol volume fractions. This behavior is indicated by a vertical dotted line at the 10% methanol volume fraction and a curved connecting line (··—··).

speculate that the influences of methanol at higher volume fractions can be attributed to the phase transition of the lipid bilayer from the state of a non-interdigitated into the state of an interdigitated bilayer structure, which occurs in the case of POPC vesicles at an about 12% methanol volume fraction [36,52]. As a consequence of this phase transition, the membrane becomes progressively thinner as well as more permeable for electrolytes and, although minimally, to certain larger non-electrolyte molecules [36,53]. The thinning effect may also hinder the nystatin from aligning into a transverse intramembrane position and consequently reduce the nystatin pore-forming ability. The flaccid and elongated vesicles that were seen only for high methanol volume fractions (Fig. 8) may even indicate the formation of transmembrane pores with diameters that are large enough to enable an almost equal membrane permeability for the glucose and sucrose molecules.

5. Conclusions

The studies of the behavior of GUVs (made out of POPC) using phase-contrast microscopy and a micropipette manipulation system allow us, in contrast to many other (spectroscopic) techniques that enable only the studies on populations of SUVs and LUVs, observations on individual, cell-sized vesicles.

Vesicle shape changes and membrane formations, nonselective, transient tension pores and vesicle ruptures were revealed. They represent three characteristic features, occurring for different nystatin concentration ranges, which are related to nystatin incorporation into the phospholipid bilayer. Therefore, our observations confirm the notion that nystatin is able to form transmembrane pores in phospholipid membranes devoid of sterols.

Vesicle shape changes can be understood if the theories of vesicle shape transformations and the theory of pore formation are considered. It can be assumed that the insertion of nystatin molecules into the outer membrane monolayer increases its area compared to the inner monolayer. On the other hand, the repositioning of nystatin molecules into the membrane in a perpendicular direction and their self-aggregation with the pore formation decreases the area difference between lipid monolayers. This area difference determines the shape of a vesicle.

Both the formation of transient tension pores and vesicle ruptures, which can be interpreted as graded and "all-or-none" type permeabilization mechanisms, and the contrast dissipation associated with them, can be explained as a consequence of the size-selective channel formation by nystatin molecules in the membrane and the resulting osmotic phenomena. This allowed us to explain a two-stage model of nystatin membrane permeabilization, presented elsewhere [30], by a single mechanism.

The study of cross-interactions between nystatin and methanol, commonly used as a cosolvent in nystatin solutions, has shown that they are insignificant for methanol volume fractions of less than 10%. However, mutually antagonizing effects were observed at higher volume fractions, leading to significantly decreased nystatin pore-forming efficiency. These effects could be attributed to the phase transition of the lipid bilayer from the state of non-interdigitated into the state of an interdigitated bilayer structure at higher methanol volume fractions.

Acknowledgements

We want to thank V. Arrigler for the help in the laboratory and the preparations of the phospholipid vesicles. This work was financially supported by the Slovenian Research Agency grant P1-0055.

Appendix A. Supplementary data

Supplementary data to this article can be found online at doi:10.1016/j.bbamem.2011.11.036.

References

[1] J. Bolard, How do the polyene macrolide antibiotics affect the cellular membrane properties? Biochim. Biophys. Acta 864 (1986) 257–304.
[2] S. Hartsel, J. Bolard, Amphotericin B: new life for an old drug, Trends Pharmacol. Sci. 17 (1996) 445–449.
[3] M.A. Ghannoum, L.B. Rice, Antifungal agents: mode of action, mechanisms of resistance and correlation of these mechanisms with bacterial resistance, Clin. Microbiol. Rev. 12 (1999) 501–517.
[4] C.P. Schaffner, Polyene macrolides in clinical practice: pharmacology and other adverses effects, in: S. Omura (Ed.), Macrolide Antibiotics: Chemistry, Biology and Practice, second ed., Academic Press, New York, 2002, pp. 457–507.
[5] A.J. Carrillo-Munoz, G. Quindos, C. Tur, M.T. Ruesga, Y. Miranda, O. del Valle, P.A. Cossum, T.L. Wallace, In-vitro antifungal activity of liposomal nystatin in comparison with nystatin, amphotericin B cholesteryl sulphate, liposomal amphotericin B, amphotericin B lipid complex, amphotericin B desoxycholate, fluconazole and itraconazole, J. Antimicrob. Chemother. 44 (1999) 397–401.
[6] S. Arikan, L. Ostrosky-Zeichner, M. Lozano-Chiu, V. Paetznick, D. Gordon, T. Wallace, J.H. Rex, In vitro activity of nystatin compared with those of liposomal nystatin, amphotericin B and fluconazole against clinical *Candida* isolates, J. Clin. Microbiol. 40 (2002) 1406–1412.
[7] F. Offner, V. Krcmery, M. Boogaerts, C. Doyen, D. Engelhard, P. Ribaud, C. Cordonnier, B. de Pauw, S. Durrant, J. Marie, P. Moreau, H. Guiot, G. Samonis, R. Sylvester, R. Herbrecht, the EORTC invasive fungal infections group, Liposomal nystatin in patients with invasive aspergillosis refractory to or intolerant of amphotericin B, Antimicrob. Agents Chemother. 48 (2004) 4808–4812.
[8] G. Gomišček, J. Majhenc, V. Arrigler, U. Langel, U. Soomets, S. Svetina, M. Zorko, B. Žekš, Effect of transportan on giant phospholipid vesicles, Life sciences, Book of abstracts, , 2000, p. 176.
[9] S.C. Hartsel, C. Hatch, W. Ayenew, How does amphotericin B work? Studies on model membrane systems, J. Liposome Res. 3 (1993) 377–408.
[10] A. Coutinho, M. Prieto, Cooperative partition model of nystatin interaction with phospholipid vesicles, Biophys. J. 84 (2003) 3061–3078.
[11] N. Akaike, N. Harata, Nystatin perforated patch recording and its applications to analyses of intracellular mechanisms, Jpn. J. Physiol. 44 (1994) 433–473.
[12] T.E. Andreoli, V.W. Dennis, A.M. Weigl, The effect of amphotericin B on the water and nonelectrolyte permeability of thin lipid membranes, J. Gen. Physiol. 53 (1969) 133–156.
[13] R. Holz, A. Finkelstein, The water and nonelectrolyte permeability induced in thin lipid membranes by the polyene antibiotics nystatin and amphotericin B, J. Gen. Physiol. 56 (1970) 125–145.
[14] D. Gottlieb, I.I. Carter, J.I.I. Sloneker, A. Amman, Protection of fungi against polyene antibiotics by sterols, Science 128 (1958) 361–365.
[15] J.O. Lampen, E.R. Morgan, A. Slocum, P. Arnow, Absorption of nystatin by microorganism, J. Bacteriol. 78 (1959) 282–289.
[16] S.C. Kinsky, Effect of polyene antibiotics on protoplast of *Neurospora crassa*, J. Bacteriol. 83 (1962) 351–358.
[17] G. Wiessmann, G. Sessa, The action of polyene antibiotics on phospholipids–cholesterol structures, J. Biol. Chem. 42 (1967) 616–625.
[18] J.M.T. Hamilton-Miller, Chemistry and biology of polyene macrolide antibiotics, Bacteriol. Rev. 37 (1973) 166–196.
[19] T.E. Andreoli, The structure and function of amphotericin B-cholesterol pores in lipid bilayer membranes, Ann. N. Y. Acad. Sci. 235 (1974) 448–468.
[20] B. de Kruijff, W.J. Gerritsen, R.A. Demel, Polyene antibiotic-sterol interactions in membranes of *Acholeplasma laidlawii* cells and lecithin liposomes, III. Molecular structure of the polyene antibiotic-cholesterol complexes, Biochim. Biophys. Acta 339 (1974) 57–70.
[21] P. van Hoogevest, B. de Kruijff, Effect of amphotericin B on cholesterol-containing liposomes of egg phosphatidylcholine and didocoseneoylphosphatidylcholine, A refinement of the model for the formation of pores by amphotericin B in membranes, Biochim. Biophys. Acta 511 (1978) 397–407.
[22] C.C. Hsu Chen, D.S. Feingold, Polyene antibiotic action on lecithin liposomes: effect of cholesterol and fatty acyl chains, Biochem. Biophys. Res. Commun. 51 (1973) 972–978.
[23] A. Marty, A. Finkelstein, Pores formed in lipid bilayer membranes by nystatin, differences in its one-sided and two-sided action, J. Gen. Physiol. 65 (1975) 515–526.
[24] K. Hąc-Wydro, P. Dynarowicz-Łątka, Interaction between nystatin and natural membrane lipids in Langmuir monolayers—The role of a phospholipid in the mechanism of polyenes mode of action, Biophys. Chem. 123 (2006) 154–161.
[25] K. Hąc-Wydro, J. Kapusta, A. Jagoda, P. Wydro, P. Dynarowicz-Łątka, The influence of phospholipid structure on the interactions with nystatin, a polyene antifungal antibiotic: A Langmuir monolayer study, Chem. Phys. Lipids 150 (2007) 125–135.
[26] A. Vertut-Croquin, J. Bolard, M. Chabbert, C. Gary-Bobo, Differences in the interaction of polyene antibiotic amphotericin B with cholesterol or ergosterol-containing phospholipid vesicles, A circular dichroism and permeability study, Biochemistry 22 (1983) 2939–2944.
[27] B.V. Cotero, S. Rebolledo-Antunez, I. Ortega-Blake, On the role of sterol in the formation of the amphotericin B channel, Biochim. Biophys. Acta 1375 (1998) 43–51.
[28] G. Fujii, J.-E. Chang, T. Coley, B. Steere, The formation of amphotericin B ion channels in lipid bilayers, Biochemistry 36 (1997) 4959–4968.
[29] B.E. Cohen, Amphotericin B toxicity and lethality: a tale of two channels, Int. J. Pharm. 162 (1998) 95–106.
[30] A. Coutinho, L. Silva, A. Fedorov, M. Prieto, Cholesterol and ergosterol influence nystatin surface aggregation: relation to pore formation, Biophys. J. 87 (2004) 3264–3276.
[31] L. Silva, A. Coutinho, A. Fedorov, M. Prieto, Nystatin-induced lipid vesicle permeabilization is strongly dependent on sterol structure, Biochim. Biophys. Acta 1758 (2006) 452–459.

[32] K.L. Koster, Y.P. Lei, M. Anderson, S. Martin, G. Bryant, Effects of vitrified and non-vitrified sugars on phosphatidylcholine fluid-to-gel phase transitions, Biophys. J. 78 (2000) 1932–1946.
[33] M.I. Angelova, S. Soleau, P. Meleard, F. Faucon, P. Bothorel, Preparation of giant vesicles by external AC electric fields: kinetics and applications, Prog. Colloid Polym. Sci. 89 (1992) 127–131.
[34] F. Zernike, Phase contrast, a new method for the microscopic observation of transparent objects, Physica 9 (1942) 686–698 (first part), 975–986 (second part).
[35] M. Mally, J. Majhenc, S. Svetina, B. Žekš, Mechanisms of equinatoxin II-induced transport through the membrane of a giant phospholipid vesicle, Biophys. J. 83 (2002) 944–953.
[36] J. Zeng, K.E. Smith, L.G. Chong, Effects of alcohol-induced lipid interdigitation on proton permeability in l-α-dipalmitoylphosphatidylcholine vesicles, Biophys. J. 65 (1993) 1404–1414.
[37] R. Lipowsky, The conformation of membranes, Nature 349 (1991) 475–481.
[38] S. Svetina, Vesicle budding and the origin of cellular life, Chem. Phys. Chem. 10 (2009) 2769–2776.
[39] F.Y. Chen, M.T. Lee, H.W. Huang, Evidence for membrane thinning effect as the mechanism for peptide-induced pore formation, Biophys. J. 84 (2003) 3751–3758.
[40] H.W. Huang, F.Y. Chen, M.T. Lee, Molecular mechanism of peptide-induced pores in membranes, Phys. Rev. Lett. 92 (2004) 198304.
[41] A. Zemel, A. Ben-Shaul, S. May, Perturbation of lipid membrane by amphipatic peptides and its role in pore formation, Eur. Biophys. J. 34 (2005) 230–242.
[42] J.R. Seoane, N. Vila Romeau, J. Miñones, O. Conde, P. Dynarowicz, M. Casas, The behavior of amphotericin B monolayers at the air/water interface, Prog. Colloid Polym. Sci. 105 (1997) 173–179.
[43] K. Matsuzaki, O. Murase, N. Fujii, K. Miyajima, An antimicrobial peptide, magainin 2, induced rapid flip-flop of phospholipids coupled with pore formation and peptide translocation, Biochemistry 35 (1996) 11361–11368.
[44] M.E. Kleinberg, A. Finkelstein, Single-length and double-length channels formed by nystatin in lipid bilayer membranes, J. Membr. Biol. 80 (1984) 257–269.
[45] S.G. Schultz, A.K. Solomon, Determination of the effective hydrodynamic radii of small molecules by viscometry, J. Gen. Physiol. 44 (1961) 1189–1199.
[46] M. Mally, J. Majhenc, S. Svetina, B. Žekš, The response of giant phospholipid vesicles to pore-forming peptide melittin, Biochim. Biophys. Acta 1768 (2007) 1179–1189.
[47] M. Bloom, E. Evans, O.G. Mouritsen, Physical properties of the fluid-bilayer component of cell membranes: a perspective, Q. Rev. Biophys. 24 (1991) 293–397.
[48] E. Evans, V. Heinrich, F. Ludwig, W. Rawicz, Dynamic tension spectroscopy and strength of biomembranes, Biophys. J. 85 (2003) 2342–2350.
[49] S.C. Hartsel, S.K. Benz, S.K. Peterson, B.S. Whyte, Potassium-selective amphotericin B channels are predominant in vesicles regardless of sidedness, Biochemistry 30 (1991) 77–82.
[50] T. Ruckwardt, J. Scott, P. Scott, P. Mikulecky, S.C. Hartsel, Lipid and stress dependence of amphotericin B ion selective channels in sterol-free membranes, Biochim. Biophys. Acta 1372 (1998) 283–288.
[51] C.L. Weakliem, G. Fujii, J.-E. Chang, A. Ben-Shaul, W.M. Gelbart, Effect of tension on pore formation in drug-containing vesicles, J. Phys. Chem. 99 (1995) 7694–7697.
[52] T.J. McIntosh, R.V. McDaniel, S.A. Simon, Induction of an interdigitated gel phase in fully hydrated phosphatidylcholine bilayers, Biochim. Biophys. Acta 731 (1983) 109–114.
[53] S.A. Simon, T.J. McIntosh, Interdigitated hydrocarbon chain packing causes the biphasic transition behavior in lipid/alcohol suspensions, Biochim. Biophys. Acta 773 (1984) 169–172.